IEEE Access
Multidisciplinary ⋮ Rapid Review ⋮ Open Access Journal

Received September 25, 2020, accepted October 17, 2020, date of publication November 3, 2020, date of current version November 16, 2020.

Digital Object Identifier 10.1109/ACCESS.2020.3035662

Improvement of Milling Stable Processing Condition for a Cutter With Large Ratio of Length to Diameter

YAN XIA[1,2], YI WAN[1,2], XICHUN LUO[3], YANAN LI[1,2], JINGLONG CAO[4], QINGHUA SONG[1,2], AND ZHANQIANG LIU[1,2]

[1]Key Laboratory of High Efficiency and Clean Mechanical Manufacture, Ministry of Education, School of Mechanical Engineering, Shandong University, Jinan 250061, China
[2]National Demonstration Centre for Experimental Mechanical Engineering Education, Shandong University, Jinan 250061, China
[3]Centre for Precision Manufacturing, DMEM, University of Strathclyde, Glasgow G1 1XJ, U.K.
[4]Komatsu (Shandong) Construction Machinery Company Ltd., Jining 272073, China

Corresponding author: Yi Wan (wanyi@sdu.edu.cn)

This work was supported in part by the National Natural Science Foundation of China under Grant 51975336, in part by the Key Research and Development Program of Shandong Province under Grant 2019JZZY010112, in part by the Key Basic Research Project of Natural Science Foundation of Shandong Province under Grant ZR2018ZB0106, and in part by the China Scholarship Council.

ABSTRACT In order to machine complex box and shell structures, the cutter with large ratio of length to diameter is usually used, whereas the low rigidity of the cutter hinders the increase of the stable machining parameters. This article develops one kind of damping cutter to improve the stable processing condition in this milling operation. The influences of modal characteristic of the cutter on chatter stability are investigated, where it is proven that increasing the dynamic stiffness can efficiently extend the stable zone. On this basis, two damping cutters are designed by inlaying the strips and damping core into the toolholder body. The influences of geometrical parameters and material property of the damping cutters on modal characteristics are theoretically analyzed, and the optimal geometrical dimensions are determined using the finite element simulation. Then, the two damping cutters are fabricated. After modal tests and milling machining experiments, the measured results validate the effectiveness of the developed damping cutters in terms of improvement of the stability frontier.

INDEX TERMS Milling cutter, ratio of length to diameter, variable cross sections, chatter stability, loss factor.

NOMENCLATURE

a	Axial cutting depth
a_{lim}	Limit axial cutting depth
c_x, k_x	Damping and stiffness along x direction
c_y, k_y	Damping and stiffness along y direction
d	Dynamic stiffness
e	Elastic modulus ratio
D_1, E_1	Diameter and elastic modulus of the toolholder body
D_2, E_2	Diameter and elastic modulus of the damping core
$(EI)_w$	Equivalent bending stiffness
$(EI)_1$	Bending stiffness of the toolholder body and the strips
$(EI)_2$	Bending stiffness of the damping core
$f(t)$	Dynamic milling force
f_x, f_y	Dynamic milling forces along x and y directions respectively
$F(t)$, F_0	Milling forces, and its amplitude
h	Thickness ratio
H_1, H_2	Thickness of the toolholder body and damping core
K_t	Cutting force coefficient
L	Overhang length of the cutter
m, c, k	Mass, damping, and stiffness of milling cutter
N	Teeth number
$\mathrm{w}(t)$	System response
W	Total deformation energy of the cutter.
$\Delta \mathrm{W}$	Dissipation energy by damping core

The associate editor coordinating the review of this manuscript and approving it for publication was Ming Luo.

β	Material loss factor
η	Loss factor
λ	Eigenvalue
ν	Frequency ratio
ω	Rotational frequency
ω_n	Natural frequency
(t)	Vibration displacement
$\Phi(i\omega)$	Transfer function
ψ	Phase angle
Ω	Spindle speed
$[A_0]$	Average directional coefficient matrix

I. INTRODUCTION

Chatter is a harmful self-excited vibration, which directly affects the surface quality of the machined workpiece, and even damages the machine tool and cutter [1]. So far, there have been a considerable amount of literature on chatter control. Considering whether it is real-time, the existing methods can be classified into two kinds, i.e. in-process and out-of-process strategies [2].

The essence of the in-process strategy is to detect and identify the occurrence of chatter and then to adjust the cutting parameters so as to achieve the chatter-free machining process [3]. This strategy generally contains online chatter detection and active control method. Due to the advantages of high efficiency and high accuracy, online chatter detection has been widely investigated [4]–[10]. Various signals are used to identify chatter, such as force signal [4], [5], acceleration signal [6], [7], and sound signal [8]. After signal acquisition, the feature extraction is vital to precisely detect chatter, where many relative signal processing methods, mainly including variational mode decomposition [8], continuous wavelet transform [9], and convolutional neural network [10], are proposed. However, multiple sensors, signal acquisition and processing system, and other auxiliary devices are required, which hinder the wide application of chatter detection. On the other hand, the active control method becomes increasingly important in the field of chatter control thanks to its efficiency and flexibility [11]–[14]. Accordingly, many active devices are designed, such as electromagnetic actuator [12], piezoelectric actuator [13], and magnetorheological fixture [14]. However, these devices usually need the relative elements of monitoring, identification and execution, which make this method complex and costly.

As opposed to in-process strategy, the out-of-process strategy is easy to implement. Stability prediction is a commonly effective way to avoid chatter, in which the predicted stability chart can guide the selection of the suitable machining parameters [15]. Many solutions are proposed to calculate the stability chart, such as the discretization method [16]–[18] and the frequency method [19]. As the input parameters, the precise dynamic parameters and cutting force coefficient of the machining system are crucial to predict the stability chart. However, these parameters are not constant due to the time-varying characteristic of the machining process, which has negative effect on the stability prediction [20]. With the aim to suppress chatter better, the passive control method is proposed, whose essence is to improve the machining stability through introducing an additional device that can consume vibration energy or break the regeneration effect [3]. The designed passive equipment is mainly composed of the friction damper, vibration absorber, tuned mass damper, constrained layer damper, coating damping, and nonstandard cutter. For instance, Madoliat *et al.* [21] placed the core and multi-fingered cylinder into the axial hold of a slender end milling tool to dissipate energy by the way of the friction. The dynamic vibration absorber with variable stiffness was designed and was filled into a boring bar, where the vibration reduction performance was verified by experiments [22]. A passive damper was developed and was embedded into a milling cutter to achieve the chatter control [23]. According to the constrained layer damping beam theory, the different damping toolholders were separately proposed, and were used in boring, milling and turning operations [24]–[26]. Fu *et al.* [27] applied the multi-layered nanostructures of carbon on the surface of milling tools to improve the vibration damping, thus increasing the stability limit. Mei *et al.* [28] designed the milling cutters with alternating variable pitches to improve the machining stability. In addition, Wan *et al.* [29] proposed a stability improvement method through applying the tensile prestress to the thin-walled piece.

From the above references reviewed, even though the chatter control has been explored broadly, the milling dynamics has received very little attention with regard to the cutter with large ratio of length to diameter and variable cross sections. Therefore, the motivation of this article is to study the dynamics of this kind of milling cutter, and then to design the novel damping cutter, thereby improving the machining stability.

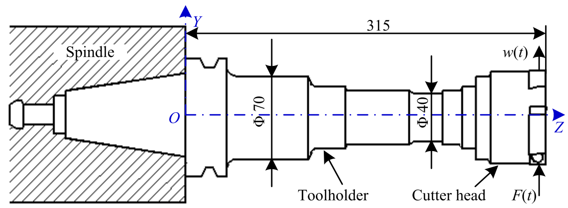

FIGURE 1. **Schematic diagram of milling cutter. (The dimension units are mm).**

II. DYNAMIC MODEL OF MILLING CUTTER

As shown in Fig. 1, the milling cutter includes a cutter head and a toolholder with the long overhang and variable cross sections. Supposing the positioning connection between the spindle and the toolholder is rigid, the milling cutter can be regarded as the cantilever structure with one end fixed and another end free.

During milling operation, the end free is subjected to the milling force. Note that the axial force along z direction is neglected, since it has little effect on the radial displacement. The cutter can be simplified as a cutter-spring-damper system. The milling forces attached on cutter head and the

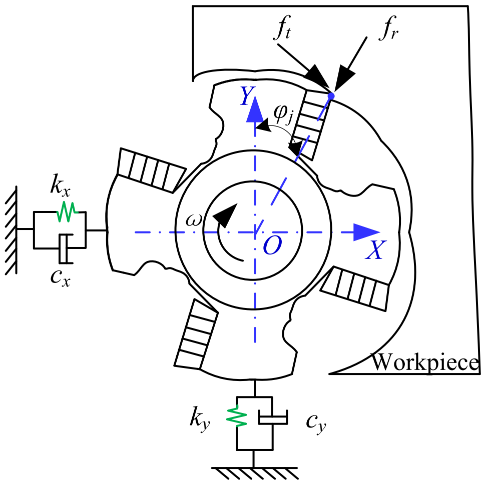

FIGURE 2. Dynamic model of milling cutter system.

corresponding displacement can meet the requirement of the following equation:

$$m\ddot{w}(t) + c\dot{w}(t) + kw(t) = F(t) \tag{1}$$

where m, c and k are mass, damping and stiffness of the cutter separately, $F(t)$ is the exciting force produced from the cutting process, and w(t) refers to the response along x or y direction. The damping c can be described as follows:

$$c = \eta\sqrt{km} \tag{2}$$

where η represents the loss factor.

Then, the system response can be obtained from Eq. (1), which is expressed as:

$$w(t) = \frac{F_0}{k} \cdot \frac{1}{\sqrt{(1-\nu^2)^2 + (\eta\nu)^2}} e^{i(\omega t - \psi)} \tag{3}$$

where F_0 represents the amplitude of $F(t)$, $\nu = \omega/\omega_{\mathrm{n}}$ is the frequency ratio, ω_{n} stands for the natural frequency, ψ is the phase angle. According to Eq. (3), it can be qualitatively obtained that the vibration displacement can be decreased with the increase of k and η. In order to further analyze the relation between the vibration response of the machining system and its modal characteristic in detail, the dynamic stiffness d [25] is defined and is expressed as:

$$d = \eta \cdot k \tag{4}$$

According to the dynamics theory of the milling operation [19], the cutter in Fig. 1 and workpiece can be expressed as a vibration system during milling process, as seen in Fig. 2.

Since the dynamic milling force $f(t)$ of $F(t)$ only affects the chatter stability, $f(t)$ is thus described as

$$\{\mathbf{f}(t)\} = \frac{1}{2}aK_t\,[\mathbf{A}_0]\,\{\mathbf{\Delta}(t)\} \tag{5}$$

with

$$\mathbf{f}(t) = \left\{\mathbf{f}_x \quad \mathbf{f}_y\right\}^T \quad \mathbf{\Delta}(t) = \{\Delta x(t) \quad \Delta y(t)\}^T \tag{6}$$

where a refers to the cutting depth, $[\mathbf{A}_0]$ is the average directional coefficient matrix, Kt is the cutting force coefficients, and $\Delta(t)$ represents the variation of vibration displacements.

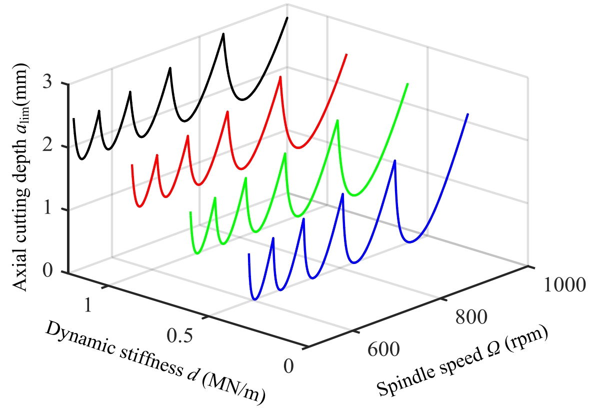

FIGURE 3. Stability charts among dynamic stiffness, spindle speed, and axial cutting depth.

Transforming Eq. (5) from time domain to frequency domain leads to:

$$\{\mathbf{f}(\omega)\} = \frac{1}{2}aK_t\,[\mathbf{A}_0]\,(1 - e^{-i\omega T})\,[\mathbf{\Phi}(i\omega)]\,\{\mathbf{f}(\omega)\} \tag{7}$$

with

$$[\mathbf{\Phi}(i\omega)] = \begin{bmatrix} \Phi_{xx}(i\omega) & 0 \\ 0 & \Phi_{yy}(i\omega) \end{bmatrix} \tag{8}$$

where $\Phi\ (i\omega)$ stands for the transfer function, and it can be described as:

$$\begin{aligned} \Phi_{xx}(i\omega) &= \frac{1}{k_x(1 - \nu^2 + i\eta_x\nu)} \\ \Phi_{yy}(i\omega) &= \frac{1}{k_y(1 - \nu^2 + i\eta_y\nu)} \end{aligned} \tag{9}$$

When around the chatter frequency, the cutter will be in the limit steady state, and the corresponding characteristic equation is derived as follows:

$$\det\left\{[\mathbf{I}] - \frac{1}{2}a_{\lim}K_t[\mathbf{A}_0](1 - e^{-i\omega_c T})[\mathbf{\Phi}(i\omega_c)]\right\} = 0 \tag{10}$$

After solving Eq. (10), the limit axial cutting depth alim and the corresponding spindle speed Ω can be given by:

$$\begin{aligned} a_{\lim} &= -\frac{2\pi}{NK_t}\left(\frac{\lambda_{\mathrm{Re}}(1-\cos(\omega_c T)) + \lambda_{\mathrm{Im}}\sin(\omega_c T)}{(1-\cos(\omega_c T))} + i\frac{\lambda_{\mathrm{Im}}(1-\cos(\omega_c T)) + \lambda_{\mathrm{Re}}\sin(\omega_c T)}{(1-\cos(\omega_c T))}\right) \\ \Omega &= \frac{60\omega_c}{N(\pi - 2\arctan(\lambda_{\mathrm{Im}}/\lambda_{\mathrm{Re}}) + 2n\pi)} \quad n = 0, 1, 2\cdots \end{aligned} \tag{11}$$

where λ is the eigenvalue, and N is the teeth number of the cutter.

Ignoring the imaginary part of Eq. (11), and then combing Eq. (4), the relation among the limit axial cutting depth $a_{\lim}$, dynamic stiffness d and spindle speed Ω can be obtained and is shown in Fig. 3. It clearly demonstrates that the limit axial cutting depth $a_{\lim}$ is significantly increased with the gradual increase of d, which is consistent with the results in [25], [29].

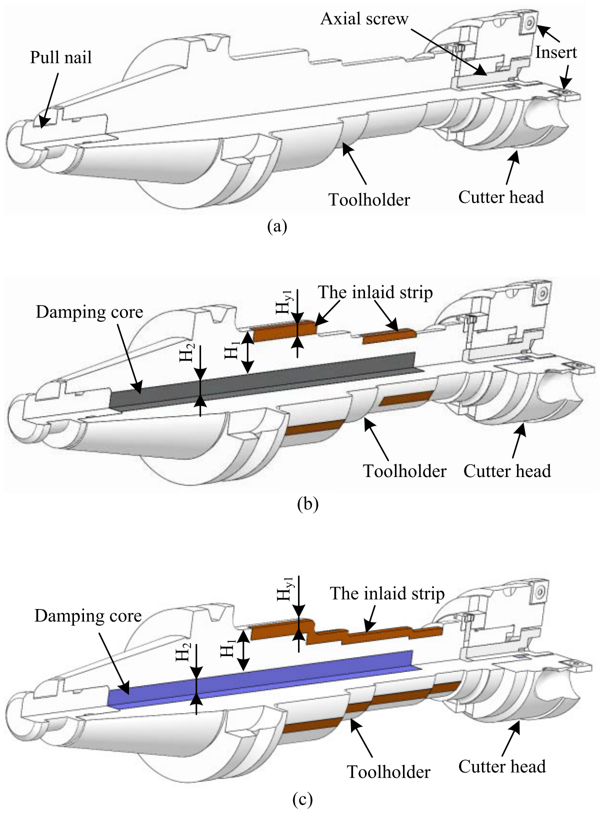

FIGURE 4. Comparison of structures for the conventional cutter (a), the damping cutter with discontinuous strips (b) and the damping cutter with continuous strips (c).

In other words, increasing the dynamics stiffness of the cutter system can improve the chatter stability.

III. DEVELOPMENT OF DAMPING CUTTER

A. DESIGN OF DAMPING CUTTER

As shown in Fig. 4a, the conventional cutter, named CC, is mainly composed of a conventional toolholder, cutter head, inserts, pull nail and axial screw. The cutter can be fixed with the spindle via the pull nail, while the cutter head with four inserts is closely connected with the toolholder by the axial screw.

Based on the above finding, two damping cutters are initially designed as shown in Figs. 4b and 4c, where they are respectively called DCDS and DCCS for analytical convenience. In Fig. 4b or Fig. 4c, a damping core is filled into the toolholder body to improve the damping performance, and the strips made of material with high modulus are embedded into the toolholder using the welding method to increase the rigidity, which can enlarge the dynamic stiffness. It should be pointed out that every strip embedded into the DCCS matches with the external shape of the toolholder, whereas the strips in the DCDS are not continuous.

The material of 35CrMo steel is used to manufacture the toolholder body. Owing to high damping performance, Foamed aluminium (FA) and Polyurethane rubber (PR) are selected as the materials of damping core in the DCDS and DCCS respectively [24], [30]. And YG6 steel is chosen to make the strip, since it has high modulus. The properties of the used materials are given in Table 1.

TABLE 1. Material properties used in cutters.

Material	Density (g/cm^3)	Elastic modulus (GPa)	Poisson's ratio	Material loss factor (%)
35CrMo	7.87	213	0.29	0.1
YG6	14.5	600	0.21	0.1
FA	0.65	12	0.33	12
PR	1.11	30	0.3	47

B. MODAL CHARACTERISTICS OF DAMPING CUTTER

To analyze the modal characteristics of the damping cutter, some assumptions are firstly provided as follows [25]: (1) the bending strains produced from damping core, strip and toolholder body show the same linear distribution in vertical direction; (2) there is not relative sliding between the contact surfaces among the above three parts; (3) the material of damping core is uniform. The stability limit of milling cutter is characterized by dynamic stiffness as shown in Fig. 3. According to the dynamic model in Fig. 1, the cutter is regarded as a cantilever structure [29], whose stiffness can be expressed as:

$$k = \frac{3(EI)_w}{L^3} \tag{12}$$

where L represents the overhang length of milling cutter, (EI)w denotes the equivalent bending stiffness which can be described as:

$$(EI)_w = (EI)_1 + (EI)_2 \tag{13}$$

where $(EI)_1$ is the bending stiffness of both toolholder body and strips, and $(EI)_2$ is the bending stiffness for the damping core.

The substitution of Eq. (13) into Eq. (12) gives:

$$k = \frac{3\pi[D_2^4 \cdot E_2 + (D_1^4 + D_2^4) \cdot E_1]}{L^3} \tag{14}$$

where E_1 and D_1 are elastic modulus and diameter for the toolholder body, and E_2 and D_2 are the elastic modulus and diameter for the damping core, respectively.

During milling operation, the cutter is suffered from the milling vibration, where the damping core can dissipate the vibration energy by the resulting bending strain. Based on the bending strain energy method [25], [31], the loss factor of the damping cutter can be represented by:

$$\eta \frac{\Delta W}{W} \tag{15}$$

where ΔW strands for the dissipation energy by damping core, and W is the total deformation energy of the cutter.

Substituting the geometrical parameter and material property of the damping cutter into Eq. (15), then the following

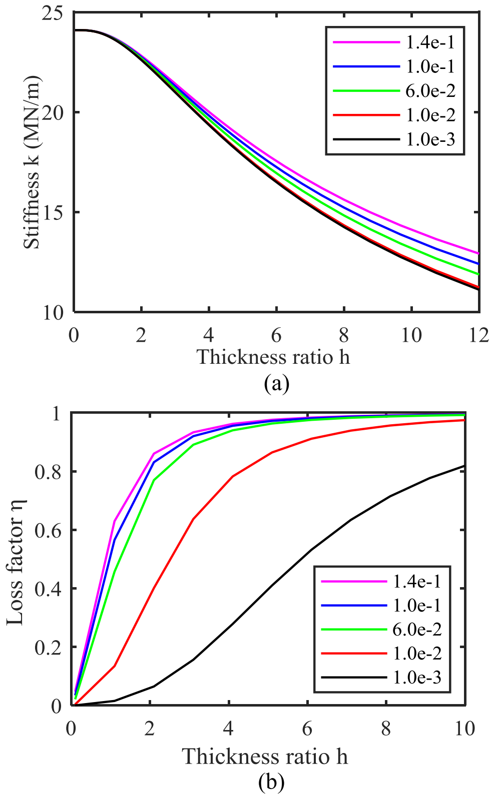

FIGURE 5. Stiffness (a) and loss factor (b) with respect to the geometrical dimension and material property.

equation can be obtained as:

$$\eta = \frac{\alpha\beta\left[H_{12}^2 + r_2^2(1+2\alpha)\right]}{\alpha H_{12}^2 + (\alpha r_2^2 + r_1^2)(1+2\alpha)} \tag{16}$$

with

$$r_1^2 = H_1^2 \big/ 12 \;\; r_2^2 = H_2^2 \big/ 12 \;\; H_{12} = (H_1 + H_2)/2$$
$$e = E_2 \big/ E_1 \;\; h = H_2 \big/ H_1 \;\; \alpha = e \cdot h \tag{17}$$

where H_1 is the thickness of the toolholder body, $H_2 = D_2/2$ is the thickness of damping core, and β is the material loss factor.

Thus, Eq. (16) can be further transformed into the following expression:

$$\eta = \frac{eh(3 + 6h + 4h^2)}{1 + eh(5 + 6h + 4h^2)} \tag{18}$$

According to Eqs. (14) and (18), the relations among the modal characteristics of the damping cutter, its geometrical dimension and material property are shown in Fig. 5, where the toolholder section with the diameter of 70 mm is selected. When h increases, i.e. increasing the diameter of damping core, the stiffness gradually decreases, whereas the loss factor is remarkably enhanced. The e of large value has a positive effect on the modal characteristic. Apparently, when FA and PR are selected for the damping core, that is, e are equal to 0.06 and 0.14, respectively, which demonstrate well damping performance as shown in Fig. 5b. However, it is difficult to obtain the suitable structural parameters for the strips and damping core from the qualitative theory analysis, since the cross sections of the cutter are variable. Therefore, the finite element method (FEM) is employed to determine the optimum dimensions for the damping cutter in the next subsection.

TABLE 2. Optimal design parameters.

Number	Cutter	Design parameters	
		H_{y1} (mm)	H_2(mm)
1	CC	-	-
2	DCDS	10.26	15.45
3	DCCS	7.35	18.14

C. PARAMETER OPTIMIZATION AND MANUFACTURE OF DAMPING CUTTER

As seen in Fig. 4, the thicknesses of the inlaid strip and the diameter of the damping core, i.e., H_{y1} and H_2, are selected as the design variables. For convenience of the optimization analysis, the thicknesses of the strips embedded into the different cross sections of the toolholder body are proportional to the corresponding diameters of the cross sections. The optimization goal is to make the maximum response amplitude of the cutter head smallest.

The basic flow of the optimization analysis mainly includes: firstly creating the input and output channels in the cutter head, then setting the design variable and optimization goal, further conducting the optimized analysis by goal driven optimization, and finally achieving the solutions. The obtained optimal parameters for the two damping cutters are listed in Table 2. The corresponding dynamic stiffness and the response amplitudes for the three cutters are demonstrated in Fig. 6. It can be found that the dynamic characteristic of the DCDS is better than of the conventional cutter, while the dynamic performance of the DCCS is better than that of the DCDS.

According to the optimal design parameters, the two damping cutters are manufactured as shown in Fig. 7, where the dynamic balance tests for the damping cutters are performed to meet the good rotation precision.

IV. PERFORMANCE TESTS AND COMPARISON

In order to verify the chatter stability of the damping cutters developed above, modal testing and milling experiments are conducted on a CNC machining center (SPN50R) in the workshop of KSD. Before milling tests, the modal parameters of the machining system are measured by modal testing to predict the stability chart, and simultaneously is used to verify the above simulated modal characteristic. The used cutter head with the diameter of 80 mm has four inserts. The material of ductile cast iron is used to make workpiece.

A. MODAL TESTING

During modal testing, the hammer (CL-YD-303) with the sensitivity of 4.29 pC/N and accelerometer sensor

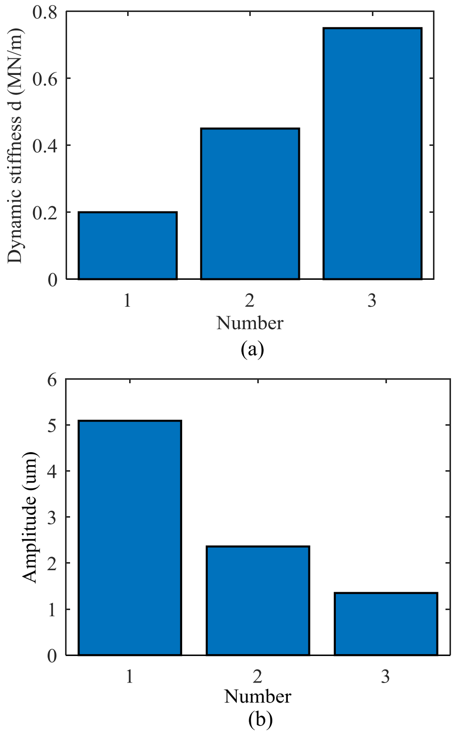

FIGURE 6. The simulated dynamic stiffness (a) and response amplitude (b) for the CC, DCDS and DCCS.

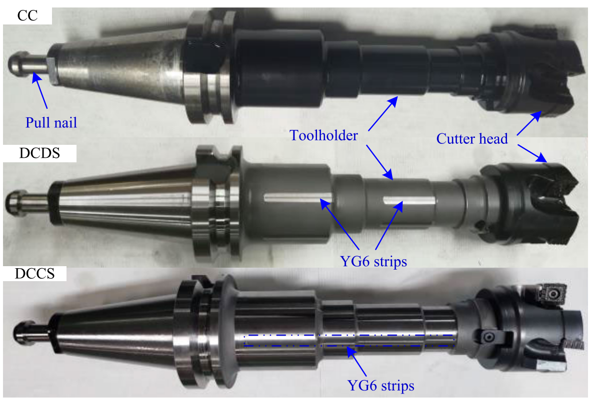

FIGURE 7. Photographs of the CC, DCDS and DCCS.

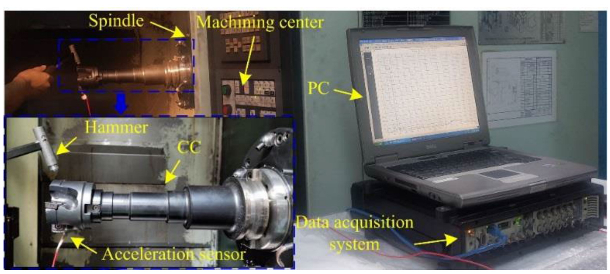

FIGURE 8. Experimental setup for modal testing.

(Dytran 3035B) are employed as shown in Fig. 8. The hammer provides the impact forces at cutter head and synchronously the responses signals are collected by B&K Pulse 3560C data acquisition system.

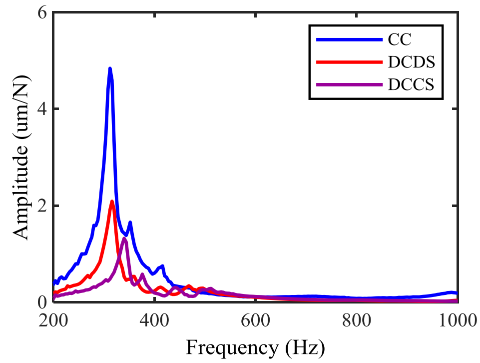

FIGURE 9. Measured frequency curves of the CC, DCDS and DCCS.

TABLE 3. Measured modal parameters of three cutters.

Modal parameters	CC	DCDS	DCCS
Natural frequency (Hz)	312	316	340
Damping ratio (%)	1.28	2.53	2.35
Stiffness (MN/m)	8.07	9.3	16.08
Dynamic stiffness (MN/m)	0.21	0.47	0.76

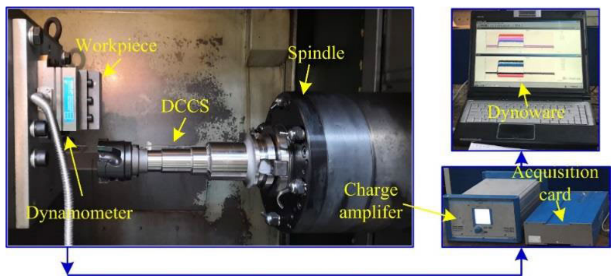

FIGURE 10. Experimental setup for milling force testing.

The measured frequency curves along y direction for three milling cutters are illustrated in Fig. 9, where the modal characteristic along x direction can be considered to be same with that along y direction because of the symmetrical structure. The corresponding modal parameters are identified and given in Table 3, which experimentally shows the obvious improvement of dynamic stiffness for the damping cutters, especially the DCCS, compared with the conventional cutter. In addition, the measured results verify that the simulated results from the FEM is effective under the range of the errors permitted.

B. FACE MILLING EXPERIMENTS

Fig. 10 presents the cutting experimental setup. The workpiece is mounted on the dynamometer (Kistler 9257B) fixed on the vertical machine table. During milling process, the milling forces can be measured to detect the cutting state. When the conventional cutter is used in workshop, the relative machining parameters include the spindle speed of 796 rpm, axial depth of cut of 1.5 mm, and feed rate of 31 mm/min. In order to compare the machining stability for the CC, DCDS

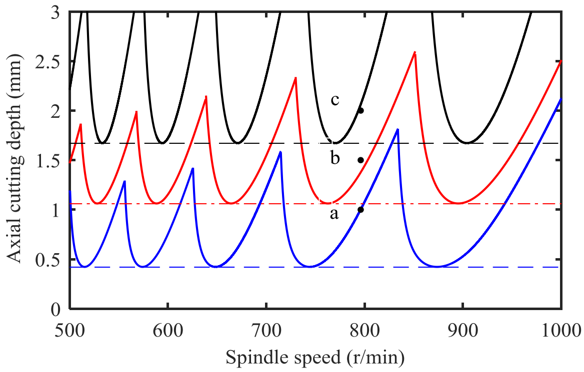

FIGURE 11. Stability charts for the CC, DCDS and DCCS.

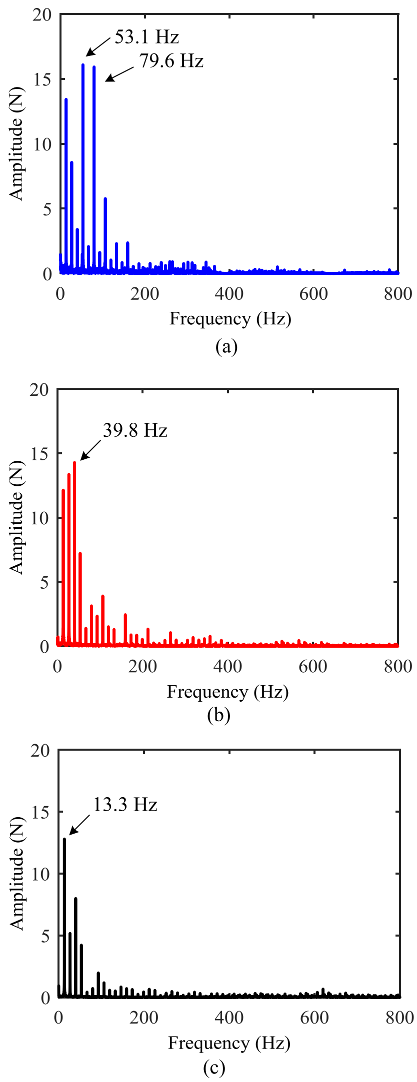

FIGURE 12. Milling force in frequency domain under $a = 1.0$ mm when using the CC (a), DCDS (b) and DCCS (c), respectively.

and DCCS, three axial cutting depths from 1 mm to 2 mm at the 0.5 mm intervals are chosen as shown in Fig. 11, and other machining parameters are constant. Thus, under the different axial depth of cut, the milling forces from the three cutters are

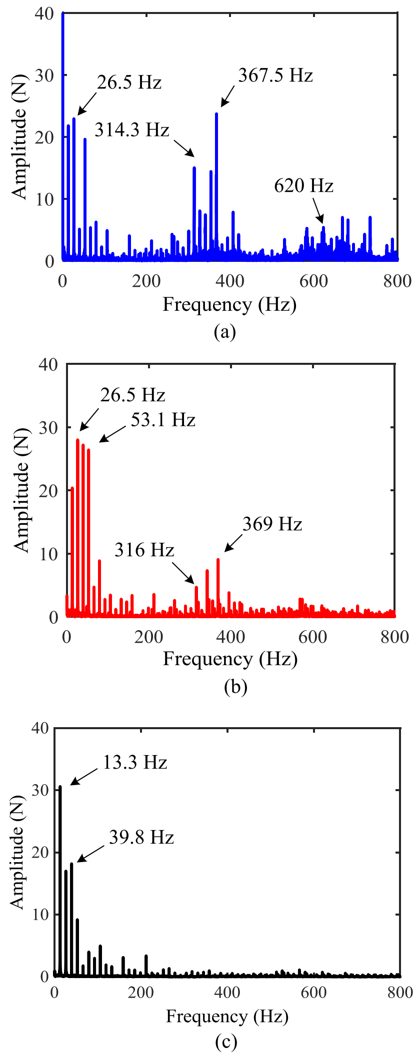

FIGURE 13. Milling force in frequency domain under $a = 1.5$ mm when using the CC (a), DCDS (b) and DCCS (c), respectively.

measured during milling process, whose spectra are presented in Figs. 12-14 in detail to reveal the machining stable state.

When the axial cutting depth is equal to 1 mm, i.e. point a in Fig. 11, the rotational frequency (13.27 Hz) and its multiplication frequencies (39.8 Hz, 53.1 Hz, 79.6 Hz,…) are the dominant frequency in Fig. 12 whether the damping cutters are used or not. This always means that the milling state is stable by using the conventional or damping cutters.

As the axial cutting depth reaches to 1.5 mm in point b, complex frequencies appear in Figs. 13a and 13b. Specifically, the vibration responses gather around 314.3 Hz and 367.5 Hz in Fig. 13a when using the conventional cutter. These frequencies are approximatively expressed by 314 Hz and 314 Hz plus 4 times of rotational frequency, where frequency value 314 Hz is near to the natural frequency along y direction. In other words, the responses near the natural frequency are dominant, which means the occurrence of chatter. Similarly, it can be found in Fig. 13b that the chatter also appears when using the DCDS, whereas the vibration

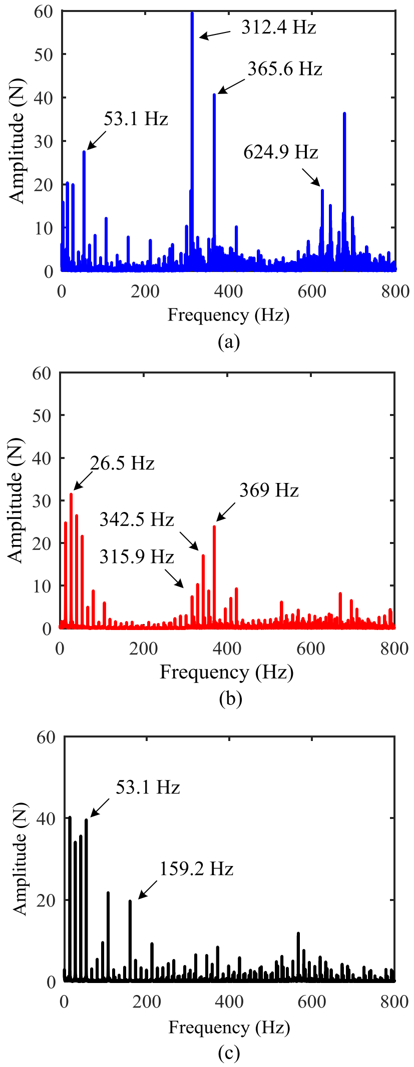

FIGURE 14. **Milling force in frequency domain under $a = 2.0$ mm when using the CC (a), DCDS (b) and DCCS (c), respectively.**

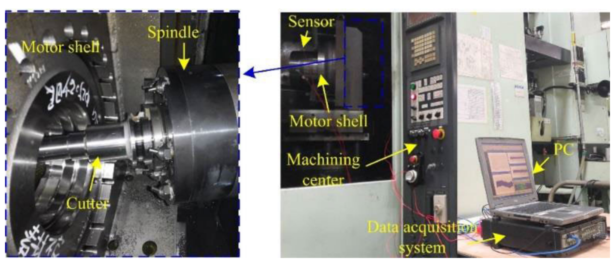

FIGURE 15. **Vibration acceleration signal acquisition setup when machining the motor shell.**

amplitude is much less than that in Fig. 13a. When the DCCS is used, the milling process is still stable as shown in Fig. 13c. The axial depth of cut further increases to 2 mm in point c. Compared to Figs. 13a and 13b, both of the chatter phenomenon in Figs. 14a and 14b becomes serious when using the CC and DCDS. Additionally, it shows the slight unstable in Fig. 14c when DCCS is used, where some complex frequencies appear. Under the different axial depths of cut,

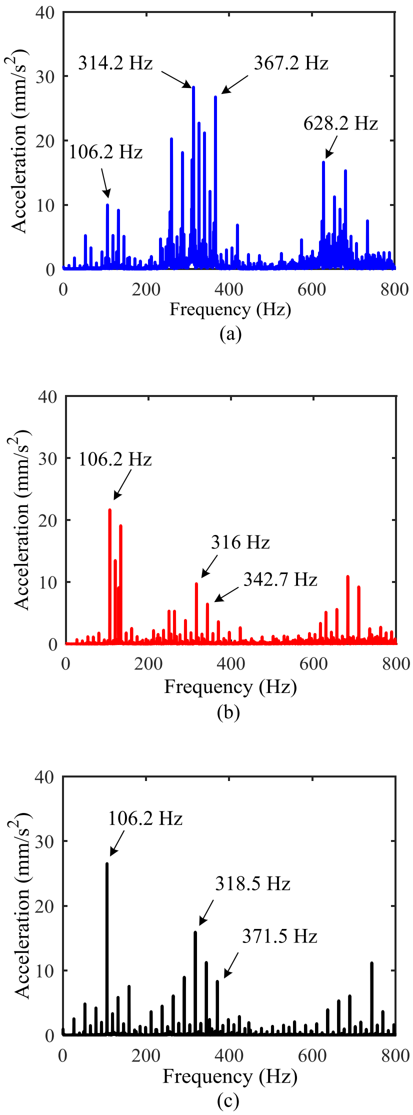

FIGURE 16. **Vibration acceleration responses under $a = 1.5$ mm when using the CC (a), DCDS (b) and DCCS (c), respectively.**

the machining state shows various forms. The measured results show that the developed damping cutters, especially the DCCS, can improve the stable machining parameters obviously.

In order to further compare the machining performance, the damping cutters are then used to machine the motor shell in workshop as shown in Fig. 15. The cutting parameters of the conventional cutter used in workshop are selected. The corresponding acceleration responses are acquired via the acceleration sensor during milling process. The measured results are shown in Fig. 16. It can be found that the chatter occurs when using the CC and DCDS, whereas the amplitude in Fig. 16b is far below that in Fig. 16a. From Fig. 16c, the machining state is stable when using the DCCS. These imply that the chatter stability performance in the order from high to low is the DCCS, DCDS and CC.

V. CONCLUSION

In this article, the novel damping cutter is proposed to improve the stable zone of the milling cutter with large overhang and variable cross sections. The dynamic model for the cutter system is built to reveal the effect of the stiffness and loss factor on the chatter stability. According to the passive control strategy, two damping cutters are designed by embedding the strips and damping core into the toolholder body, whose modal characteristics analysis shows that the geometrical dimension and damping materials have the direct effects on the dynamic performance. Through the optimization analysis, the optimal geometrical dimensions are determined and then the damping cutters are manufactured. Modal testing is carried out to compare the dynamic characteristic of the conventional and damping cutters, and the measured dynamic stiffness for the proposed cutter with 0.47 MN/m or 0.76 MN/m is much larger than that of the conventional cutter with 0.21 MN/m. The predicted stability charts for three cutters are verified by the cutting tests. Compared with the conventional cutter, the stability performance is improved significantly when using the damping cutters. It is worth noting that the designed damping cutters have been practically applied in the workshop of KSD.

ACKNOWLEDGMENT

The authors are grateful for the support from Komatsu (Shandong) Construction Machinery Company Ltd., in the damping cutter manufacture and experiments.

REFERENCES

[1] Y. Liu, D. Zhang, and B. Wu, "An efficient full-discretization method for prediction of milling stability," *Int. J. Mach. Tools Manuf.*, vol. 63, pp. 44–48, Dec. 2012.

[2] G. Quintana and J. Ciurana, "Chatter in machining processes: A review," *Int. J. Mach. Tools Manuf.*, vol. 51, no. 5, pp. 363–376, May 2011.

[3] C. Yue, H. Gao, X. Liu, S. Y. Liang, and L. Wang, "A review of chatter vibration research in milling," *Chin. J. Aeronaut.*, vol. 32, no. 2, pp. 215–242, Feb. 2019.

[4] K. Li, S. He, B. Li, H. Liu, X. Mao, and C. Shi, "A novel online chatter detection method in milling process based on multiscale entropy and gradient tree boosting," *Mech. Syst. Signal Process.*, vol. 135, Jan. 2020, Art. no. 106385.

[5] Z. Zhang, H. Li, G. Meng, X. Tu, and C. Cheng, "Chatter detection in milling process based on the energy entropy of VMD and WPD," *Int. J. Mach. Tools Manuf.*, vol. 108, pp. 106–112, Sep. 2016.

[6] P. Albertelli, L. Braghieri, M. Torta, and M. Monno, "Development of a generalized chatter detection methodology for variable speed machining," *Mech. Syst. Signal Process.*, vol. 123, pp. 26–42, May 2019.

[7] B.-L. Jian, C.-C. Wang, J.-Y. Chang, X.-Y. Su, and H.-T. Yau, "Machine tool chatter identification based on dynamic errors of different self-synchronized chaotic systems of various fractional orders," *IEEE Access*, vol. 7, pp. 67278–67286, May 2019.

[8] C. Liu, L. Zhu, and C. Ni, "Chatter detection in milling process based on VMD and energy entropy," *Mech. Syst. Signal Process.*, vol. 105, pp. 169–182, May 2018.

[9] M.-Q. Tran, M.-K. Liu, and Q.-V. Tran, "Milling chatter detection using scalogram and deep convolutional neural network," *Int. J. Adv. Manuf. Technol.*, vol. 107, nos. 3–4, pp. 1505–1516, Mar. 2020.

[10] W. Zhu, J. Zhuang, B. Guo, W. Teng, and F. Wu, "An optimized convolutional neural network for chatter detection in the milling of thin-walled parts," *Int. J. Adv. Manuf. Technol.*, vol. 106, nos. 9–10, pp. 3881–3895, Jan. 2020.

[11] S. Paul and R. Morales-Menendez, "Active control of chatter in milling process using intelligent PD/PID control," *IEEE Access*, vol. 6, pp. 72698–72713, Nov. 2018.

[12] S. Wan, X. Li, W. Su, J. Yuan, J. Hong, and X. Jin, "Active damping of milling chatter vibration via a novel spindle system with an integrated electromagnetic actuator," *Precis. Eng.*, vol. 57, pp. 203–210, May 2019.

[13] S. Wang, Q. Song, and Z. Liu, "Vibration suppression of thin-walled workpiece milling using a time-space varying PD control method via piezoelectric actuator," *Int. J. Adv. Manuf. Technol.*, vol. 105, nos. 7–8, pp. 2843–2856, Nov. 2019.

[14] X. Jiang, G. Zhao, and W. Lu, "Vibration suppression of complex thin-walled workpiece based on magnetorheological fixture," *Int. J. Adv. Manuf. Technol.*, vol. 106, nos. 3–4, pp. 1043–1055, Jan. 2020.

[15] H. Merrit, "Theory of self-excited machine-tool chatter-contribution to machine tool chatter research-1," *ASME J. Eng. Ind.*, vol. 87, no. 4, pp. 447–454, Nov. 1965.

[16] T. Insperger and G. Stépán, "Updated semi-discretization method for periodic delay-differential equations with discrete delay," *Int. J. Numer. Methods Eng.*, vol. 61, no. 1, pp. 117–141, Sep. 2004.

[17] Y. Ding, L. Zhu, X. Zhang, and H. Ding, "A full-discretization method for prediction of milling stability," *Int. J. Mach. Tools Manuf.*, vol. 50, no. 5, pp. 502–509, May 2010.

[18] Y. Ding, L. Zhu, X. Zhang, and H. Ding, "Second-order full-discretization method for milling stability prediction," *Int. J. Mach. Tools Manuf.*, vol. 50, no. 10, pp. 926–932, May 2010.

[19] Y. Altintas, G. Stepan, D. Merdol, and Z. Dombovari, "Chatter stability of milling in frequency and discrete time domain," *CIRP J. Manuf. Sci. Technol.*, vol. 1, no. 1, pp. 35–44, 2008.

[20] C. Wang, X. Zhang, J. Liu, R. Yan, H. Cao, and X. Chen, "Multi harmonic and random stiffness excitation for milling chatter suppression," *Mech. Syst. Signal Process.*, vol. 120, pp. 777–792, Apr. 2019.

[21] R. Madoliat, S. Hayati, and A. Ghasemi Ghalebahman, "Investigation of chatter suppression in slender endmill via a frictional damper," *Scientia Iranica*, vol. 18, no. 5, pp. 1069–1077, Oct. 2011.

[22] X. Liu, Q. Liu, S. Wu, R. Li, and H. Gao, "Analysis of the vibration characteristics and adjustment method of boring bar with a variable stiffness vibration absorber," *Int. J. Adv. Manuf. Technol.*, vol. 98, nos. 1–4, pp. 95–105, Sep. 2018.

[23] Y. Yang, Y. Wang, and Q. Liu, "Design of a milling cutter with large length–diameter ratio based on embedded passive damper," *J. Vib. Control*, vol. 25, no. 3, pp. 506–516, Jul. 2018.

[24] Q. Song, J. Shi, Z. Liu, Y. Wan, and F. Xia, "Boring bar with constrained layer damper for improving process stability," *Int. J. Adv. Manuf. Technol.*, vol. 83, nos. 9–12, pp. 1951–1966, Apr. 2016.

[25] Y. Liu, Z. Liu, Q. Song, and B. Wang, "Development of constrained layer damping toolholder to improve chatter stability in end milling," *Int. J. Mech. Sci.*, vol. 117, pp. 299–308, Oct. 2016.

[26] Y. Liu, Z. Liu, Q. Song, and B. Wang, "Analysis and implementation of chatter frequency dependent constrained layer damping tool holder for stability improvement in turning process," *J. Mater. Process. Technol.*, vol. 266, pp. 687–695, Apr. 2019.

[27] Q. Fu, G. S. Lorite, M. M.-U. Rashid, T. Selkälä, J. Uusitalo, G. Toth, K. Kordas, T. Österlind, and C. M. Nicolescu, "Suppressing tool chatter with novel multi-layered nanostructures of carbon based composite coatings," *J. Mater. Process. Technol.*, vol. 223, pp. 292–298, Sep. 2015.

[28] J. Mei, M. Luo, J. Guo, H. Li, and D. Zhang, "Analytical modeling, design and performance evaluation of chatter-free milling cutter with alternating pitch variations," *IEEE Access*, vol. 6, pp. 32367–32375, May 2018.

[29] M. Wan, T.-Q. Gao, J. Feng, and W.-H. Zhang, "On improving chatter stability of thin-wall milling by prestressing," *J. Mater. Process. Technol.*, vol. 264, pp. 32–44, Feb. 2019.

[30] D. G. Lee, H. Yun Hwang, and J. Kook Kim, "Design and manufacture of a carbon fiber epoxy rotating boring bar," *Compos. Struct.*, vol. 60, no. 1, pp. 115–124, Apr. 2003.

[31] J. H. Yim, S. Y. Cho, Y. J. Seo, and B. Z. Jang, "A study on material damping of 0° laminated composite sandwich cantilever beams with a viscoelastic layer," *Compos. Struct.*, vol. 60, no. 4, pp. 367–374, Jun. 2003.

YAN XIA received the M.S. degree from Northeastern University, China, in 2017. He is currently pursuing the Ph.D. degree with the School of Mechanical Engineering, Shandong University, China.

His current research interests include milling dynamics and vibration control.

YI WAN received the Ph.D. degree from Shandong University, China, in 2006.

Since 2015, he has been a Professor with the School of Mechanical Engineering, Shandong University. His main research interests include machining dynamics, 3D printing, and control of robot.

XICHUN LUO received the Ph.D. degree in ultraprecision manufacturing from the Harbin Institute of Technology, China, in 2002, and the Ph.D. degree in precision engineering from Leeds Metropolitan University, U.K., in 2004.

He is currently a Professor of ultraprecision manufacturing and the Technical Director of the Centre for Precision Manufacturing, University of Strathclyde, Glasgow. His research interests include ultraprecision machining, micromachining, and nanomanufacturing.

YANAN LI received the B.E. degree in mechanical design, manufacturing, and automation from the Shandong University of Science and Technology, Qingdao, China, in 2016. He is currently pursuing the M.S. degree in mechanical engineering with Shandong University, Jinan, China.

His research interest includes the abnormal behavior recognition of security robot.

JINGLONG CAO received the M.S. degree from the Shandong University of Science and Technology, Qingdao, China, in 2014. He currently works with Komatsu (Shandong) Construction Machinery Company Ltd., Jining, China. His main research interests include machining processing optimization and processing automation.

QINGHUA SONG received the M.S. and Ph.D. degrees in mechanical engineering from Shandong University, in 2003 and 2009, respectively.

Since 2019, he has been a Professor with the School of Mechanical Engineering, Shandong University. His research interests include structural vibration control, cutting system dynamics, and biomedical machinery.

ZHANQIANG LIU received the B.S. and M.S. degrees in mechanical engineering from Shandong University, in 1994, and the Ph.D. degree from the City University of Hong Kong, in 1999.

Since 2002, he has been a Professor with the School of Mechanical Engineering, Shandong University. His research interests include machining theory and tool technology.